



HAL
open science

How to prevent pressure oscillations in multicomponent flow calculations : a quasi conservative approach

Remi Abgrall

► **To cite this version:**

Remi Abgrall. How to prevent pressure oscillations in multicomponent flow calculations : a quasi conservative approach. RR-2372, INRIA. 1994. inria-00074304

HAL Id: inria-00074304

<https://inria.hal.science/inria-00074304>

Submitted on 24 May 2006

HAL is a multi-disciplinary open access archive for the deposit and dissemination of scientific research documents, whether they are published or not. The documents may come from teaching and research institutions in France or abroad, or from public or private research centers.

L'archive ouverte pluridisciplinaire **HAL**, est destinée au dépôt et à la diffusion de documents scientifiques de niveau recherche, publiés ou non, émanant des établissements d'enseignement et de recherche français ou étrangers, des laboratoires publics ou privés.

*How to prevent pressure oscillations in
multicomponent flow calculations : a quasi
conservative approach*

Rémi ABGRALL

N° 2372

Octobre 1994

PROGRAMME 6

Calcul scientifique,
modélisation
et logiciel numérique



*Rapport
de recherche*

1994

How to prevent pressure oscillations in multicomponent flow calculations : a quasi conservative approach

Rémi ABGRALL *

Programme 6 — Calcul scientifique, modélisation et logiciel numérique
Projet Sinus

Rapport de recherche n° 2372 — Octobre 1994 — 19 pages

Abstract: A new numerical scheme for computing multicomponent flows is presented. It is able to handle strong shocks, is pressure oscillation free through the contact discontinuities and guaranties the positivity of mass fractions. Some numerical experiments on shock tubes indicate the convergence to the correct weak solution. Comparisons with classical finite volume schemes are also proposed.

Key-words: Godunov-type schemes, multicomponent flows

(Résumé : tsvp)

*abgrall@sophia.inria.fr

Comment ne pas avoir d'oscillations de pression dans les simulations numériques d'écoulements compressibles multi-espèces : une approche quasi conservative

Résumé : On présente un nouveau schéma numérique permettant le calcul d'écoulements multi-espèces. Il est capable de simuler des chocs forts, garantit l'absence d'oscillations au travers des lignes de glissement et garantit la positivité des fractions massiques. Quelques expériences sur des tubes à choc indiquent la convergence vers les bonnes solutions faibles du problème, bien que ce schéma ne soit pas strictement conservatif. On propose aussi des comparaisons avec des schémas volumes finis classiques

Mots-clé : Schémas de type Godunov, écoulements multi-espèces

In this paper, we are interested in the simulation of multicomponent non reacting flows. The thermodynamical assumptions are :

- the gas is a mixture of ns calorically perfect gases Σ_i . Their equation of state is

$$\epsilon_i = \rho_i c_{v_i} T \quad (1)$$

where ϵ_i is the internal energy of the species Σ_i , ρ_i is its density, T is the temperature and the specific heat c_{v_i} is independent of T ,

- the pressure is given by Dalton's law.

Without loss of generality, we may assume that $ns = 2$.

This kind of problem has already been widely studied, see [7, 6, 5, 4] for example. The classical finite volume type of schemes are usually faced with two major difficulties : the mass fractions Y and $1 - Y$ may become negative, the pressure may present oscillations through contact discontinuities, instead of remaining continuous. These difficulties are intimately related to their "finite volume" nature.

Let us describe some remedies.

Positivity A modification of the numerical flux introduced by Larrouturou [5] enables to guaranty the positivity of mass fractions under a CFL like condition. This modification does not prevent pressure oscillations [1].

Pressure S. Karni has introduced a non conservative scheme that enable to properly simulate the contact discontinuities (see [3, 4]). The positivity of mass fraction is also guaranteed. The conservation errors are controlled but this scheme cannot handle strong shocks. The conservations errors become so large that the solution no longer converges to the right one. See Hou and Le Floch [8] for a study of this kind of problems.

1 Problem description

The internal energy of each species Σ_i follows (1) thus the total internal energy is

$$\epsilon = \rho c_v T \quad (2)$$

where $\rho = \rho^{(1)} + \rho^{(2)}$ and

$$c_v = Y^{(1)}c_{v1} + Y^{(2)}c_{v2}.$$

The relation between the pressure p and the internal energy is

$$p = (\gamma - 1)\epsilon \quad (3)$$

where

$$\gamma = \frac{Y^{(1)}c_{p1} + Y^{(2)}c_{p2}}{Y^{(1)}c_{v1} + Y^{(2)}c_{v2}} \quad (4)$$

As usual, we have set $c_{p1} = \gamma_i c_{vi}$. We often denotes $\gamma - 1$ by κ . The total energy per unit volume is

$$E = \epsilon + \frac{1}{2}\rho u^2,$$

here u is the velocity.

Several equivalent sets of partial differential equation may be considered for this model. They are written as

$$\frac{\partial W}{\partial t} + \frac{\partial F(W)}{\partial x} = 0$$

and have the same weak solutions.

1. Symmetric formulation ([6] for example)

$$W = \begin{pmatrix} \rho^{(1)} \\ \rho^{(2)} \\ \rho u \\ E \end{pmatrix} \quad F(W) = \begin{pmatrix} \rho^{(1)}u \\ \rho^{(2)}u \\ \rho u^2 + p \\ u(E + p) \end{pmatrix} \quad (5)$$

2. Unsymmetric formulation ([5, 4] for example)

$$W = \begin{pmatrix} \rho \\ \rho Y \\ \rho u \\ E \end{pmatrix} \quad F(W) = \begin{pmatrix} \rho u \\ \rho Y u \\ \rho u^2 + p \\ u(E + p) \end{pmatrix} \quad (6)$$

3. “Gamma” formulation ([7] for example)

$$W = \begin{pmatrix} \rho \\ \rho\gamma \\ \rho u \\ E \end{pmatrix} \quad F(W) = \begin{pmatrix} \rho u \\ \rho\gamma u \\ \rho u^2 + p \\ u(E + p) \end{pmatrix} \quad (7)$$

4. $\frac{1}{\gamma-1}$ formulation

$$W = \begin{pmatrix} \frac{\rho}{\gamma-1} \\ \rho u \\ E \end{pmatrix} \quad F(W) = \begin{pmatrix} \frac{\rho u}{\gamma-1} \\ \rho u^2 + p \\ u(E + p) \end{pmatrix} \quad (8)$$

These four formulations are equivalent since γ is an homographic function of the mass fractions.

The major drawback of the finite volume formulations, that can be rewritten (in their first order version) as

$$W^{n+1} = P . E . W^n,$$

is not the evolution operator E (since even when it is exact, the same problem on the pressure exists) but lies in the projection operator P . To illustrate this, let us consider the system (5) for a supersonic contact discontinuity so that the scheme reduces to

$$W_i^{n+1} = W_i^n - \lambda [F(W_{i+1}^n) - F(W_i^n)].$$

What follows is valid for any finite volume numerical scheme. We assume for the sake of simplicity that the pressure is uniform ($p_j^n = p$, for all j) as well as the velocity ($u_j^n = u$). As it is shown in [6] and systematically exploited in [1], the first iteration of the scheme preserves the velocity u but the value of p_i^{n+1} is different of p . In [4], the same kind of analysis is done for the Roe scheme adapted to various multicomponent models.

The explanation is the following. The evolution of partial densities, momentum and energy are independent. The pressure is obtained through the

energy by γ , the density and the momentum. The value of γ is computed from those of $\rho^{(1)}$ and $\rho^{(2)}$. The four conserved quantities are average of the exact values in the cells. Thus the value of γ is an ‘‘averaged’’ value that does not correspond the value that would have been needed to preserve the pressure. Once the pressure is wrong in one cell, the velocity will go wrong at the next time step, and so on. The situation is more or less serious, depending on the initial conditions. Quirk and Karni [2] give an example where the numerical solution has few to do with the exact one. It can be easily understood that in combustion or detonation problems, the presence of a stiff source term can amplify this deficiency.

In [4], this problem is solved by using a non conservative formulation of the Euler equation with primitive variables. S. Karni notices that the evolution of p only depends, in this formulation, on the gradients of p and u . Since they vanishes through a contact discontinuity, p should remain constant.

In what follows, we show how to modify a finite volume scheme in order to prevent pressure oscillations. We illustrate this technique when Roe’s Riemann solver is employed. We show the first order and second order version of this scheme. We show that it is robust enough to handle strong discontinuities. We show by comparing the solutions with the exact one that mesh convergence to the propre weak solution is indeed reached.

2 General principle, first order version of the scheme

We start from the first order upwind scheme

$$W_i^{n+1} = W_i^n - \lambda [F_{i+1/2} - F_{i-1/2}].$$

The numerical flux $F_{i+1/2} = F(W_i, W_{i+1})$ is given by Roe’s linearization :

$$F(W_L, W_R) = \frac{1}{2} [F(W_L) + F(W_R) - |\bar{A}| (W_R - W_L)].$$

In what follows the formulation (5) is considered. The matrix \bar{A} depends on $\bar{Y}^{(1)}$, $\bar{Y}^{(2)}$, \bar{u} , \bar{H} , $\bar{\chi}_j = \frac{\partial p}{\partial \rho_j}$ ($j = 1, 2$) and $\bar{\kappa} = \frac{\partial p}{\partial \epsilon}$. They have the following

values

$$\overline{Y^{(j)}} = \frac{\sqrt{\rho_L}Y_L^{(j)} + \sqrt{\rho_R}Y_R^{(j)}}{\sqrt{\rho_L} + \sqrt{\rho_R}} \quad j = 1, 2$$

$$\overline{u} = \frac{\sqrt{\rho_L}u_L + \sqrt{\rho_R}u_R}{\sqrt{\rho_L} + \sqrt{\rho_R}}$$

$$\overline{H} = \frac{\sqrt{\rho_L}H_L + \sqrt{\rho_R}H_R}{\sqrt{\rho_L} + \sqrt{\rho_R}}$$

The value of $\overline{\kappa}$ is given by (4) where $Y^{(1)}$ and $Y^{(2)}$ are replaced by the corresponding average values defined above. Those of $\overline{\chi_i}$ are defined by

$$\Delta p = \overline{\chi_1}\Delta\rho^{(1)} + \overline{\chi_2}\Delta\rho^{(2)} + \overline{\kappa}\Delta\epsilon, \quad (9)$$

we have set $\Delta\rho^{(j)} = \rho_L^{(j)} - \rho_R^{(j)}$, etc, to simplify the notations.

Assume now that the three states $W_{i+1}^n, W_i^n, W_{i-1}^n$ have the same pressure p and the same velocity u . A straightforward calculation shows that, if one sets

$$\Delta_{i+1/2} = \rho_{i+1} - \rho_i \quad \Delta'_{i+1/2} = \frac{1}{\kappa_{i+1}^n} - \frac{1}{\kappa_i^n},$$

$$\Delta_{i+1/2}^{(1)} = \rho_{i+1}^{(1)} - \rho_i^{(1)} \quad \Delta_{i+1/2}^{(2)} = \rho_{i+1}^{(2)} - \rho_i^{(2)}$$

we get

$$|\overline{A_{i+1/2}}| (W_{i+1}^n - W_i^n) = \begin{pmatrix} |u|\Delta_{i+1/2}^{(1)} \\ |u|\Delta_{i+1/2}^{(2)} \\ |u|u\Delta_{i+1/2} \\ |u|\frac{u^2}{2}\Delta_{1/2} + p\Delta'_{1/2} \end{pmatrix}.$$

Here we have taken into account the relation (9) with $\Delta p = 0$.

Using all this, it is easy to see that

$$\begin{aligned}
\rho_i^{n+1} &= \rho_i^n - \lambda \left(u(\Delta_{1/2} + \Delta_{-1/2}) - |u|(\Delta_{1/2} - \Delta_{-1/2}) \right) \\
u_i^{n+1} &= u \\
E_i^{n+1} &= E_i^n - \lambda \left(\frac{u p}{2} [\Delta'_{1/2} + \Delta'_{-1/2}] - \frac{|u| u}{2} [\Delta'_{1/2} - \Delta'_{-1/2}] + \right. \\
&\quad \left. \frac{u^2}{4} [\Delta_{1/2} + \Delta_{-1/2}] - \frac{|u| u^2}{4} [\Delta'_{1/2} - \Delta'_{-1/2}] \right)
\end{aligned} \tag{10}$$

Since $E_i^n = \frac{p}{\kappa_i^n} + \frac{1}{2} \rho_i^n u^2$ and $E_i^{n+1} = \frac{p_i^{n+1}}{\kappa_i^{n+1}} + \frac{1}{2} \rho_i^{n+1} u^2$, we can see that a necessary condition for $p_i^{n+1} = p$ is

$$\frac{1}{\kappa_i^{n+1}} = \frac{1}{\kappa_i^n} - \frac{\lambda}{2} \left(u_i^n [\Delta'_{1/2} + \Delta'_{-1/2}] - |u_i^n| [\Delta'_{1/2} - \Delta'_{-1/2}] \right). \tag{11}$$

The equation (11) is nothing more than a discretization of

$$\left(\frac{1}{\kappa} \right)_t + u \left(\frac{1}{\kappa} \right)_x = 0.$$

All together, our numerical scheme is the following :

1. update of ρ , ρu and E by the classical multispecies Roe scheme,
2. update of $\frac{1}{\kappa_i^n}$ by (11). The mass fractions $Y^{(1),n+1}$ and $Y^{(2),n+1}$ are obtained by inverting (4).

Since $\frac{1}{\kappa_i^n} \in [\min_i (\frac{1}{\kappa_i^0}), \max_i (\frac{1}{\kappa_i^0})]$ if $\lambda \max_i |u_i^n| \leq 1$, the mass fractions $Y^{(1)}$ and $Y^{(2)}$ remains in $[0, 1]$ with the same CFL condition as in the original scheme.

3 High order extensions

We assume that a high order extension of the original finite volume scheme is obtained through the MUSCL method. In each cell, we get a reconstruction of the conservative variables :

$$W_i^n(x) = W_i^n + \delta W^n(x). \quad (12)$$

The slope is computed so that the average of (12) in $[x_{i-1/2}, x_{i+1/2}]$ is W_i^n . The variation $\delta W(x)$ is obtained by computing slopes either on the primitive or characteristic variables. The slope may be limited with the help of limiters, or computed with the help of the ENO method. In both cases, we assume that if all the points of the stencil used to compute δW share the same pressure p and the same velocity u , then the velocity and the pressure defined by (12) are u and p .

To simplify the text, we assume that the standard high order finite volume scheme is the following second order scheme :

$$W_i^{n+1/2} = W_i^n - \frac{\lambda}{2} \left(F(W_i^{n+}) - F(W_i^{n-}) \right) \quad (a)$$

$$W_i^{n+1} = W_i^n - \lambda \left(F(W_i^{n+1/2+}, W_{i+1}^{n+1/2-}) - F(W_{i-1}^{n+1/2+}, W_i^{n+1/2-}) \right) \quad (b)$$

$$(13)$$

Here, we have set for $l = n$ or $n + 1/2$

$$\begin{aligned} W_i^{l+} &= W_i^l + \delta W^l \left(\frac{\Delta x}{2} \right), \\ W_i^{l-} &= W_i^l + \delta W^l \left(-\frac{\Delta x}{2} \right). \end{aligned}$$

The exact flux is used in the predictor step, while the Roe flux is employed in the corrector one.

To construct our multicomponent scheme, the simplest way is to update $\frac{1}{\kappa}$ in such a way that an initial condition made of a contact discontinuity (with velocity u and pressure p) will remain a contact discontinuity. In order to simplify the text, we introduce, for any w in ρ , u and p , the following notations :

$$w_{i+1/2}^{\pm} = \begin{cases} w_i + \frac{1}{2} \delta w_i, \\ w_{i+1} - \frac{1}{2} \delta w_{i+1}. \end{cases}$$

The δw_i are computed from (12). Their expressions depend on the kind of variable we have used to define δW . According to the assumptions we have made, if at time t_n , W^n defines a contact discontinuity, and we have :

$$\begin{aligned}\rho_{i+1/2}^+ &= \rho_i^n + \frac{1}{2}\delta\rho_i & \rho_{i+1/2}^- &= \rho_{i+1}^n - \frac{1}{2}\delta\rho_{i+1} \\ u_{i+1/2}^\pm &= u_i^n = u_{i+1}^n & p_{i+1/2}^\pm &= p_i^n = p_{i+1}^n \\ \frac{1}{\kappa_{i+1/2}^+} &= \frac{1}{\kappa_i^n} + \frac{1}{2}\delta\frac{1}{\kappa_i} & \frac{1}{\kappa_{i+1/2}^-} &= \frac{1}{\kappa_{i+1}^n} - \frac{1}{2}\delta\frac{1}{\kappa_{i+1}}\end{aligned}$$

Some straightforward calculations shows that after the predictor step, the velocity remains the same and the pressure also remains invariant provided that

$$\frac{1}{\kappa_i^{n+1/2}} = \frac{1}{\kappa_i^n} - \lambda \left(\frac{1}{\kappa_{i+1/2}^+} u_{i+1/2}^+ - \frac{1}{\kappa_{i+1/2}^-} u_{i+1/2}^- \right). \quad (14)$$

Then, the same result is true after the corrector step, provided that $\frac{1}{\kappa}$ is updated by

$$\begin{aligned}\frac{1}{\kappa_i^{n+1}} &= \frac{1}{\kappa_i^n} - \frac{\lambda}{2} \left(u_i^{n+1/2} [\Delta'_{1/2} + \Delta'_{-1/2} + \delta^+] - |u_i^{n+1/2}| [\Delta'_{1/2} + \Delta'_{-1/2} - \delta^-] \right) \\ \delta^+ &= \frac{1}{2} \left(\delta_{i+1}^{n+1/2} - 2\delta_i^{n+1/2} + \delta_{i-1}^{n+1/2} \right) \\ \delta^- &= \frac{1}{2} \left(\delta_{i+1}^{n+1/2} - \delta_{i-1}^{n+1/2} \right)\end{aligned} \quad (15)$$

Our modified scheme is the following

1. Predictor step : update ρ , ρu and E by (13)-(a) and $\frac{1}{\kappa}$ by (14),
2. Corrector step : update ρ , ρu and E by (13)-(b) and $\frac{1}{\kappa}$ by (15).

The scheme is stable under the same CFL condition. The mass fractions remain positive.

4 Numerical experiments

In this section, we want to illustrate this methodology and to compare it to the existing finite volume one, and show it can handle strong shocks. We also wish to check whether the numerical solution converges to the weak one.

4.1 Comparison with finite volume schemes

We consider the following test case : The ratio of specific heats are respectively

	Y_1	ρ	u	p
Left	0	1	0	25
Right	1	1	0	0.01

Table 1: Initial conditions

1.6 and 1.1. Other test cases have been performed (in particular those of [1]) but this one provides larger discrepancies. Note that even with a constant γ , the numerical solution is far from being perfect : this test case seems to be difficult for finite volume schemes. The Figures 1, 2, 3, 4 gives the density, velocity, pressure and $\gamma - 1$ at time $t = 0.008 \lambda = 0.012$ for the first order scheme. From Figures 1 and 2, it is clear that our new volume scheme behaves much better than the classical finite volume one. In Figure 5 and 6, we present the pressure and the velocity for the same test case with the second order scheme. The reconstruction is applied on the physical variables. We also present some computational results on the Karni and Quirk's test case : It consists of a shock tube filled with air ($\gamma = 1.4, c_v = 0.72$) where a shock wave move to the right. In the pre-shock wave state, a bubble of Helium is set ($\gamma = 1.67, c_v = 2.42$). We use 200 cells, the shock wave is initially at $x = 0.25$ and the bubble sits between $x = 0.4$ and $x = 0.6$. The results are presented at time $t = 0.35$, are obtained with the second order version of both schemes with extrapolation on the characteristic variable. The CFL number is 0.75. The Figure 7-a shows the pressure obtained with the present scheme, while Figure 7-b shows what is obtained with the conservative scheme of [5]. Spurious oscillations, as with

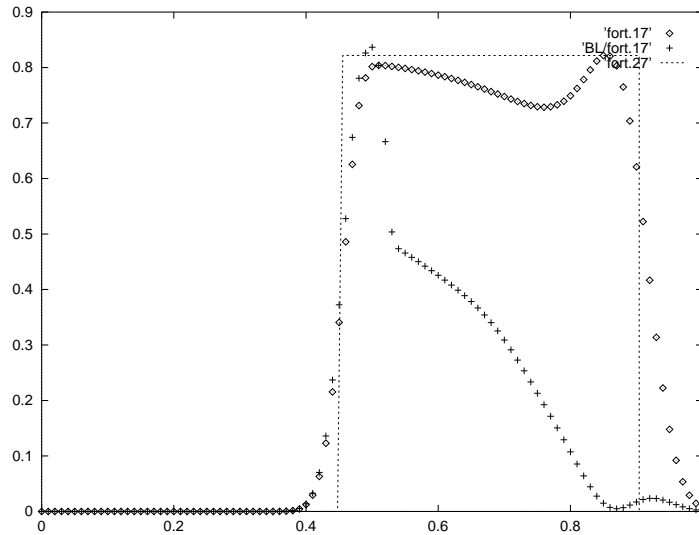


Figure 1: Velocity, 1st order. \diamond : present scheme, $+$: finite volume scheme of [5], dotted line : exact solution

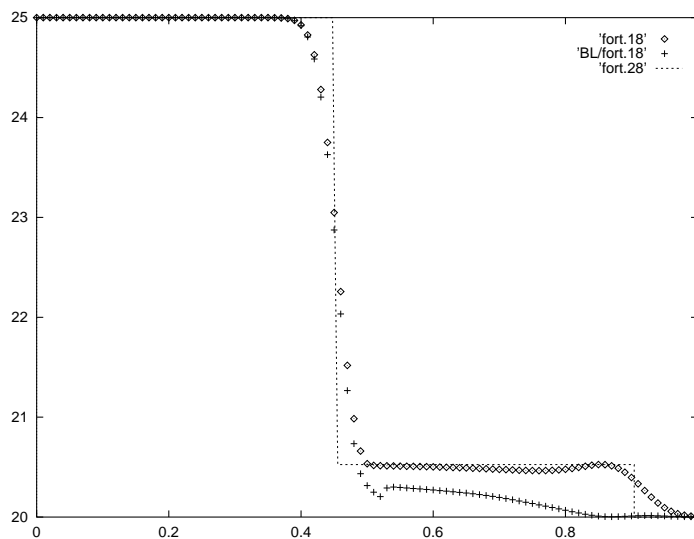


Figure 2: Pressure, 1st order \diamond : present scheme, $+$: finite volume scheme of [5], dotted line : exact solution

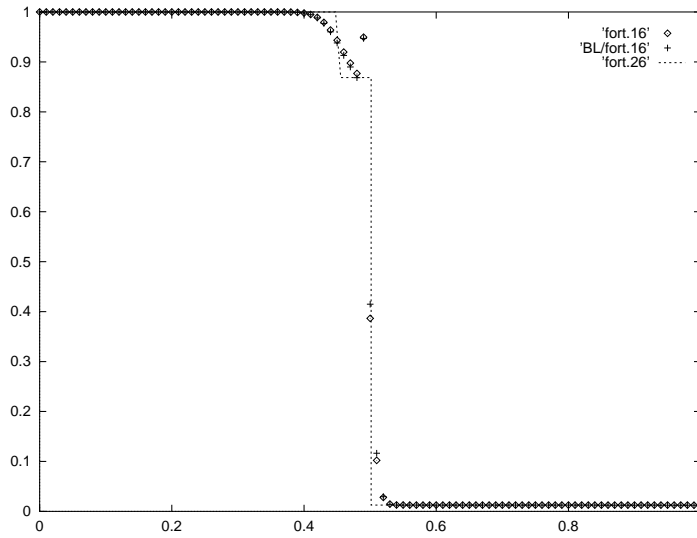


Figure 3: Density, 1st order \diamond : present scheme, + : finite volume scheme of [5], dotted line : exact solution

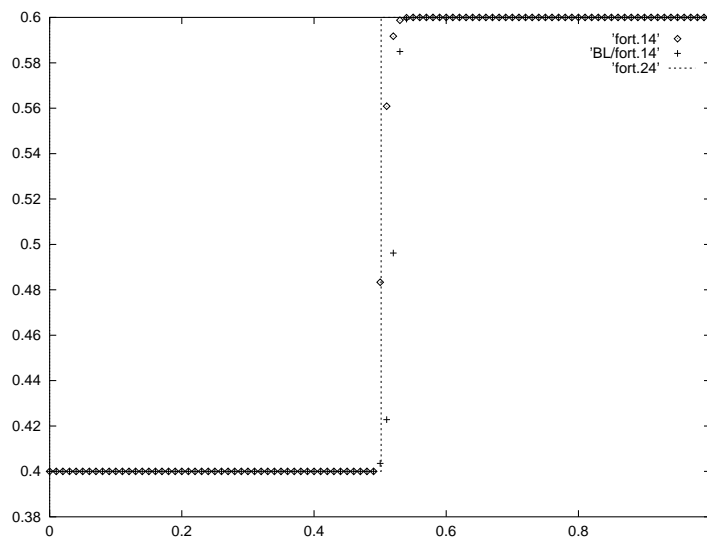


Figure 4: $\gamma - 1$, 1st order \diamond : present scheme, + : finite volume scheme of [5], dotted line : exact solution

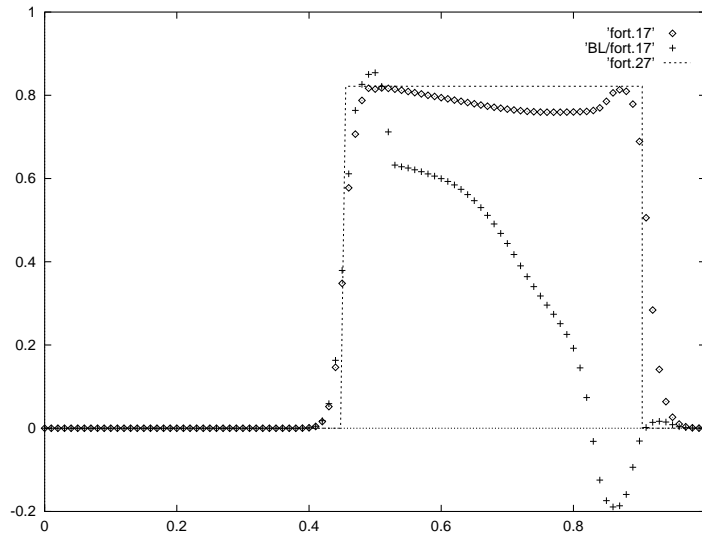


Figure 5: Velocity, 2nd order, \diamond : present scheme, $+$: finite volume scheme of [5], dotted line : exact solution

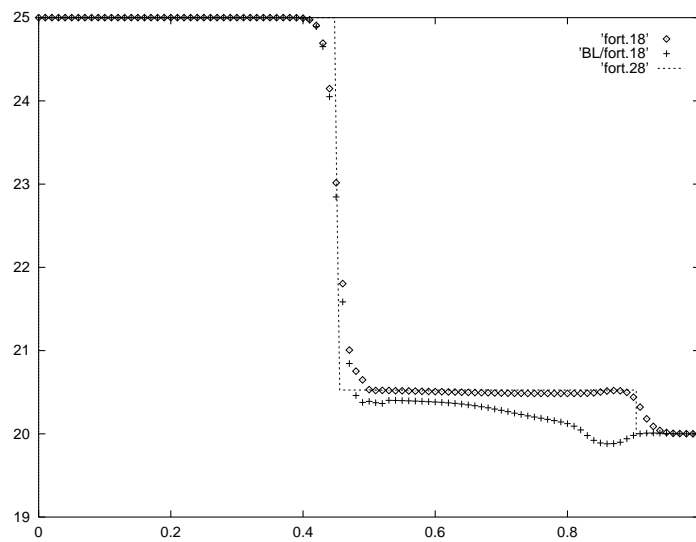


Figure 6: Pressure, 2nd order, \diamond : present scheme, $+$: finite volume scheme of [5], dotted line : exact solution

	Y_1	ρ	u	p
Post shock	1	1.3765	0.3948	1.57
Pre shock	1	1	0	1
bubble	0	0.138	0	1

Table 2: Shock/bubble interaction

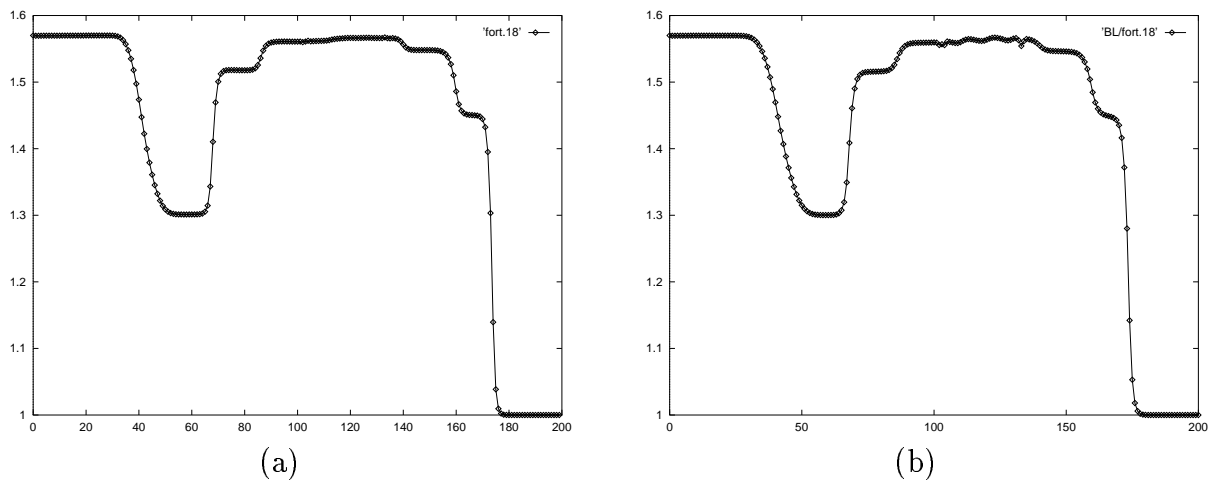


Figure 7: Pressure, 2nd order, present scheme (a), conservative scheme (b)

Quirk and Karni's results are visible for the conservative scheme and are absent for the present scheme.

We can see these Figures, that our new scheme also behave much better than the old one. This conclusion is the same whatever the test case we have run.

5 Convergence to the correct weak solution

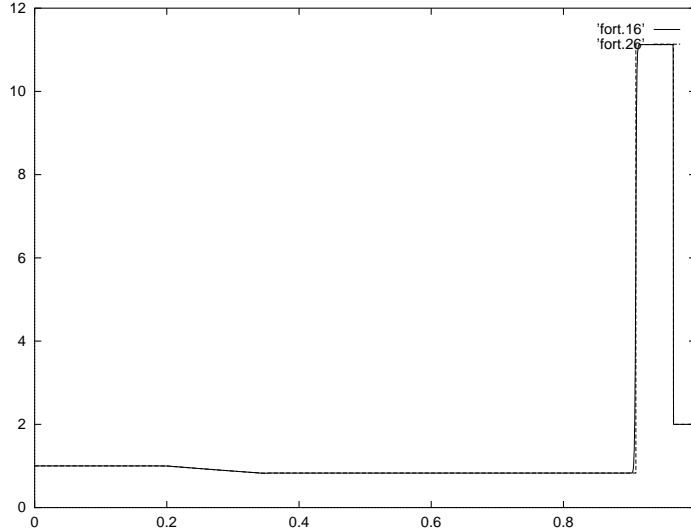


Figure 8: Density, 2nd order, 5001 mesh points, \diamond : present scheme, dotted line : exact solution

This point is studied numerically. The new scheme is tested with 5001 mesh points in its second order version (reconstruction on the primitive variables). A new test case is employed, to get stronger discontinuities. The shock Mach number (defined as $\frac{U_{shock} - u_R}{a_R}$) is 7.97, its velocity is 1.11. The contact discontinuity velocity is 0.73, its pressure is 7.40. We present the density in $[0, 1]$ (Figure 8) and a zoom (Figure 9) that enable to better the contact discontinuity and the shock wave. We clearly see that the numerical solution is very close to the exact one. In particular, the correct levels of density are obtai-

	Y_1	ρ	u	p	γ
Left	1	1	0	10	1.6
Right	0	2	-1	.1	1.4

Table 3: Initial conditions for the convergence study

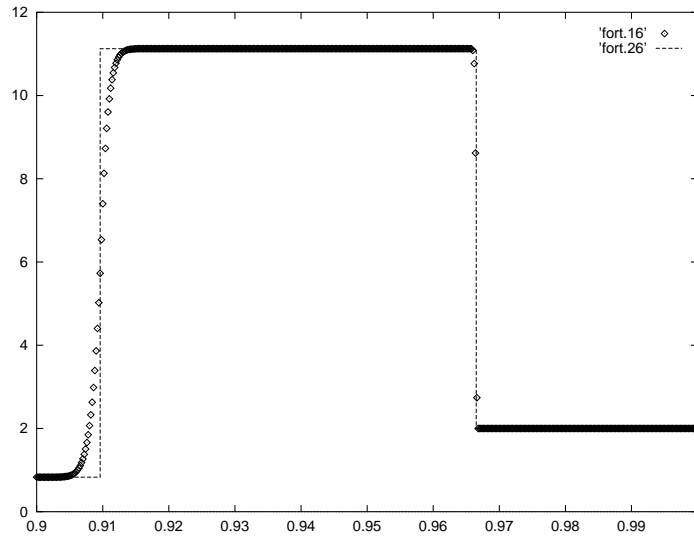


Figure 9: Zoom of the density, 2nd order, 5001 mesh points, \diamond : present scheme, dotted line : exact solution

ned, the discontinuities move at the right speed. The first conclusion is true, whatever the variable (pressure, velocity, κ or Mach number).

This conclusion is not really surprising : γ does not change in a fan or a shock wave, the present scheme is nothing more than the classical one in this case. In a contact discontinuity, the gradient of the velocity must vanish. Since we integrate simultaneously approximations of

$$\rho_t + (\rho u)_x = 0 \quad \text{and} \quad \left(\frac{1}{\kappa}\right)_t + u \left(\frac{1}{\kappa}\right)_x = 0,$$

it is legitimate to expect the right contact discontinuity speed.

6 Conclusion

We have presented a new scheme for multispecies compressible flow simulations. It is constructed to suppress or minimize the spurious oscillations that are generated by conventional finite volume schemes. This property is also true for Karni's scheme, but the present one, from its construction, is able to handle strong shocks. Extensions to more than 2 species is straightforward (consider $W = (\rho, \rho_1, \dots, \rho_{n_s-2}, \frac{1}{\kappa}, \rho u, E)$ and apply the same principles.

Acknowledgements : I would like to thanks S. Karni and J.J. Quirk for their support in this study.

References

- [1] D. Chargy, R. Abgrall, L. Fezoui et B. Larrouturou. Conservative numerical schemes for multicomponent inviscid flows. *La Recherche Aéronautique*, 2, 1992.
- [2] J.J. Quirk, S. Karni. On the dynamics of a shock-bubble interaction. Technical Report 94-75, ICASE, 1994.
- [3] S. Karni. Viscous profiles and primitive formulations. *SIAM J. Num. Anal.*, 29, 1992.

- [4] S. Karni. Multi-component flow calculations by a consistent primitive algorithm. *Journal of Computational Physics*, 112, 1994.
- [5] B. Larrouturou. How to preserve the mass fraction positivity when computing compressible multi-component flows. *Journal of Computational Physics*, 95, 1991.
- [6] R. Abgrall. Generalisation of the roe scheme for the computation of mixture of perfect gases. *la Recherche Aéronautique*, 6, Décembre 1988.
- [7] P.L. Roe. A new approach to computing discontinuous flows of several ideal gases. Technical report, Cranfield Institute of Technology, 1984.
- [8] T.Y. Hou, P. Le Floch. Why non conservative schemes converge to wrong solutions : error analysis. *Math. of Comp.*, 62(206), 1994.



Unité de recherche INRIA Lorraine, Technopôle de Nancy-Brabois, Campus scientifique,
615 rue du Jardin Botanique, BP 101, 54600 VILLERS LÈS NANCY
Unité de recherche INRIA Rennes, Irisa, Campus universitaire de Beaulieu, 35042 RENNES Cedex
Unité de recherche INRIA Rhône-Alpes, 46 avenue Félix Viallet, 38031 GRENOBLE Cedex 1
Unité de recherche INRIA Rocquencourt, Domaine de Voluceau, Rocquencourt, BP 105, 78153 LE CHESNAY Cedex
Unité de recherche INRIA Sophia-Antipolis, 2004 route des Lucioles, BP 93, 06902 SOPHIA-ANTIPOLIS Cedex

Éditeur

INRIA, Domaine de Voluceau, Rocquencourt, BP 105, 78153 LE CHESNAY Cedex (France)

ISSN 0249-6399